

# Modeling of Blood Perfusion in Dependence of Scanning Angle from LDPI Data

Jan Kubicek, Iveta Bryjova, Marek Penhaker, Vladimir Kasik, Zbynek Labza, Martin Cerny and Martin Augustynek

VSB–Technical University of Ostrava, FEECS, K450, 17. Listopadu 15, 708 33, Ostrava-Poruba, Czech Republic

Keywords: Laser, Doppler Effect, Laser Doppler, LDI, LDPI, Microcirculation, Blood Perfusion, Modeling.

Abstract: The paper deals with issue of the modelling and analysis of a scanning angle influence on the blood perfusion, and consequent proposal for their elimination. The first essential step of analysis is angle stabilization. In this step, we utilize special artificial arm allowing for a measuring angle adjustment in the scale of two axes. The modelling allows for simulation of perfusion units (PU) in the form of the quadratic model, which is consequently recalculated in the form of the linear expression. The second part of the analysis deals with the PU modelling in the dependence of the distance. In our analysis, we particularly use a segment of middle finger and forearm. In the last part, we propose theoretical conception of the curvature correction influence. This theoretical proposal leads to the relationship between measured and real PU parameter.

## 1 INTRODUCTION

For tissue activity in a cutaneous plexus, the laser method is used. The laser beam is absorbed during tissue passage, changing direction, or wavelength carrying information to the detector about erythrocytes velocity in the particular tissue. A product of the blood elements concentration with the Doppler shift of a frequency and movement velocity expresses so called number PD (Perfusion Units).

Interaction of the laser radiation with the particular tissue is influenced by the several factors: type of a tissue, optical tissue properties, wavelength, performance, power density, exposure time and in the case of a pulsed laser it is length and frequency of a pulse. Different refractive indexes in individual tissue layers and absorption level (absorption of radiation) cause different transmittance (passage of radiation), dispersion and reflection depending on the laser wavelength. (Augustynek et al., 2010), (Blazek et al., 2015), (Ida et al., 2016).

The main parameter determining penetration depth into tissue is tissue absorption calculated for given wavelength. In the case of interest of surfacing tissues, we select laser with shorter wavelength causing higher absorption with high energy

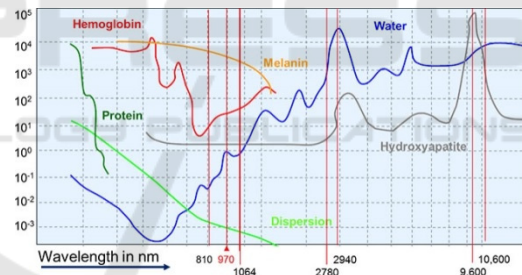


Figure 1: Laser Absorption in the dependence of wavelength. (Thieme et al., 2016)

concentration. If we do not focus on deeper structures, we select laser with wavelength below infrared area (630-750 nm). A level of laser absorption in UV area and blue spectrum induces an excitation in biomolecule where in extreme cases goes to ionization, and contrarily light with greater wavelengths causes atom oscillation, or molecule rotation around their axes manifesting in the case of thermal effects. (Brezinova et al., 2016), (Cerny et al., 2008), (Thieme et al., 2016).

## 2 MEASUREMENT OF BLOOD PERFUSION

The blood perfusion imaging by Laser Doppler Perfusion Imaging (LDPI) is a medical diagnostic imaging method which is based on the evaluation of the Doppler shift laser radiation which reflects itself from a moving blood elements typically erythrocytes by skin capillaries. This phenomenon creates the quantitative maps of the blood perfusion. This diagnostic method is frequently used in the burn medicine for the objective and non-invasive assessing of the burn trauma range and depth. By the clinical evaluation, there is up to 35% errors especially on the early stages after undergoing trauma. The correct adjusting of the thermic injuries depth is key fact for the optimization of the future diagnosis. The LDPI specificity and the sensitivity for the burn depth is determined approximately 95 %. (Bevilacqua et al., 2016), (Cerny and Penhaker., 2009), (Shin et al., 2016).

### 2.1 Scanning

Although the laser beam movement appears itself as continuous during the scanning, each measurement is in the fact created from a set of discrete points.

The maximum number of measuring points can represent matrix with dimension  $256 \times 256$ , it means that in the one image is more than 65 000 tissue points. Generally, it is appropriate to get average perfusion value along to many points because the perfusion value is suffered from noise and the spatial tissue variation in the every individual point. The spatial resolution is defined as the smallest object distance which is possible to recognize. The resolution is determined by the laser diameter (PeriScan PIM 3 allows 1 mm) and used scanning step. The highest scanning effectivity is reached in the case when the scanning step is equalled to the laser beam average. The smaller scanning step improves the visual representation of the scan but does not contribute any physiological relevant information.

Besides the perfusion scanning, PeriScan PIM 3 allows for the intensive scanning as well. This mode is constructed on the base the intensity of the laser beam back diffused to the photodetector regardless on the Doppler shift. The pixel dimensions of the intensive scan are equal as the perfusion scan. The intensive scan is useful for differentiation of the scanned object from background. (Kubicek et al., 2016), (Stetinsky et al., 2015).

The PeriScan PIM 3 also contains the built-in compensation of the signal noise from lights supplied from the standard electrical site with the frequency 50/60 Hz. The other ambient light fluctuations can also influence the measurement so that it is appropriate to ensure the stable light conditions. The light conditions influence on imaging process is the subject of this analysis. (PERIMED, 2008).



Figure 2: The arm with the head of PeriScan PIM 3. (PERIMED, 2008).

### 2.2 LDPI Software

LDPI software is the analytic tool especially intended for PeriScan systems. The software allows for to user the exact numerical overviews of the measured parameters and the color perfusion maps as well. Physician can select and highlight the region of interest (RoI) for detailed the blood perfusion assessing in the highlighted spot. (Kukucka, 2009)

The LDPI software allows for the following scanning modes:

- Single mode
- Repeated mode
- Sequential mode
- Duplex mode

The duplex mode allows the fluent measuring of the blood perfusion only in one discrete point. The measurement output is the curve of the blood perfusion dependence within the time. The sample frequency is adjusted on the 10 kHz and the sampling period is 10 ms. In the ideal case, the blood flowing plethysmography curve in the arteries is clearly observable. This phenomenon is caused by

the change flowing in the arteries which is with the scattering centers concentration the blood perfusion expressing. (Elamin et al., 2015), (Klosová et al., 2013), (Kukucka, 2009), (Machaj et al., 2016).

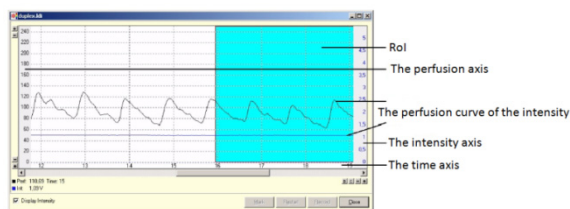


Figure 3: The measurement output in the duplex mode. The graph shows the blood perfusion dependence within the time. The RoI is indicated by blue color. The quantified blood perfusion and other records are extracted from RoI. (Elamin et al., 2015)

### 3 LDPI USING FOR DIAGNOSTIC PURPOSES

The method LDPI contributes to monitoring of the dermal plait blood perfusion. A depth of burn influences a blood perfusion, thus time needed for burn healing. On the Burn center in the university hospital in Ostrava, the system PeriScan PIM3 is used. The output represents 2D color map allowing for imaging of 256 color scale covering range of 1000 arbitrary perfusion units (PU). If perfusion rises, the color scale goes from blue to red color. Increasing blood perfusion reflects increasing skin metabolism. Patients who have undergone laser-Doppler measurement, they are classified according to tissue recovery time which is closely connected with burn level. (Basak et al., 2016), (Goei et al., 2016)

- Healing until 14 days (IIa. stage)
- Healing until 21 days (IIb. stage)
- Healing over 21 days (III. stage)

For the reason of edema in an affected area oppressing of capillaries for 48 hours after injury, instantaneous values of perfusion are distorting. (Majernik et al., 2012)

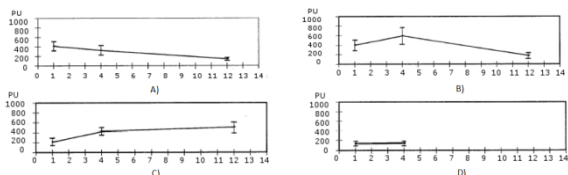


Figure 4: Perfusion change in the dependence of particular day (selected cases), (A) treatment time < 1 week, (B) treatment time < 2 weeks, (C) treatment time < 3 weeks, (D) treatment time > 3 weeks. (Schindler, 2016).

Nevertheless, it is important to start with the measurement as soon as possible. In the clinical practice, the measurement is started following day after injury. Cases when measurement exhibits in 3.-5. posttraumatic day (PTD) values greater than 147 PU, 6.-7. PTD 191 PU, 8.-9. PTD 273 PU are classified into second group. Patients with perfusion value less than 150 PU neither after 9. observed day are subjected of surgery. (Majernik et al., 2014), (Simonsen et al., 2016).

## 4 EXPERIMENTAL PART

There are two factors going to the process of measurement. The factors are divided into affected and unaffected. Each of these factors can be differentiated as examples:

- Large burn areas
- Local burn areas

In the case of large burn areas (back or stomach) – in this case of middle distance there is only affected factor of measurement. By retaining of imaginary parallelism plane of measuring head with, we bring the least possible error of the method to the measurement procedure, and measured values are slightly different from real (values are depended on distance and selected mode Low, Medium, High and Very High). It is not needed to perform a scan correction. If we change a measuring head position where laser beam is not perpendicular on surface, we bring a measurement error causing in the result unreliable perfusion values. (Penhaker et al., 2013)

Case of curved surface large burns of long bones (limbs) belongs to partially influenced case, only when burn is led in longitudinal direction with bone, and we are not focused on real values in the neighbourhood of curved surfaces. All burn areas which we cannot achieve the situation that all measured points of burned area are perpendicular to measured head are classified into unaffected cases. Our analysis is primarily aimed to purposes of unaffected measurements, but also deals with infraction of main condition of measure head parallelism in the case of affected measurement. (Marek and Krejcar, 2015), (Penhaker et al., 2011).

### 4.1 Angle Stabilization

Before approaching to the measurement, it is needed to perform of measured place angle stabilization. For this purpose, we use artificial arm (fig. 5.) allowing for an angle adjustment in two directions where it is necessary to adjust the angle scale. In the one case, it

is angle led along of edge joint (fig. 6.A), with radius 20mm (distance 90°-90° is 62.8 mm). In two cases, they are angles in the circle (fig. 6.B), with inner radius 15.5 mm and external radius 34.5 mm.



Figure 5: Detail view on the stabilizing arm with measurement angles (left), whole stabilizing arm (right).

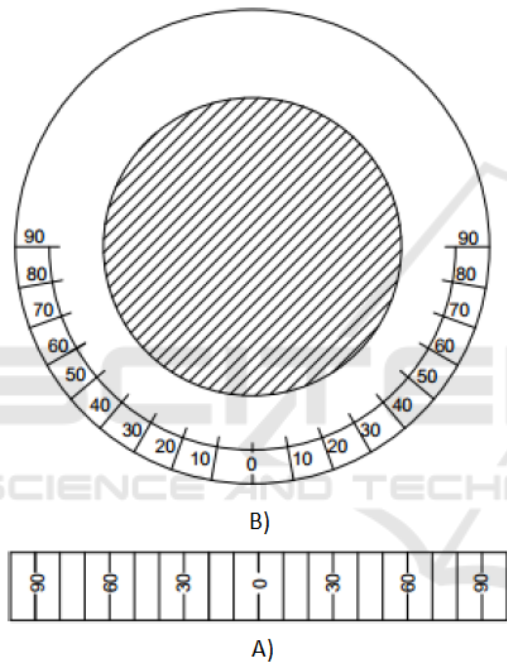


Figure 6: Used angle configuration for given radius, (B) circle configuration with inner radius 15.5 mm and external radius 34.5 mm, (A) angle led along of edge joint.

Since some of human parts do not have completely flat surface for measurement, it is needed to establish approach for placing of measured area into plane. For this purpose, we use protractor for tilt measurement. In this phase, we can approach to device calibration. Calibration is done by using of reference etalon using Brownian move.

### 4.2 Procedure of Measurement

Measurement in the single mode is carried out by the conditions summarized in (Table.1.). Single mode generates static image record, user sets scan resolution and intensity threshold. After process of

measurement, software allows for intensive and perfusion scan together with color image.

Table 1: Controlled conditions in single mode.

Atmospheric pressure	101.2 kPa
Light conditions	57 lx
Surrounding temperature	24.5 °C
Tissue temperature	36.2 °C
Humidity	32.2 °C

The output values from single mode will be used for area comparison measured under angle 50°C, and in the second case under 60°C.

Measurement in the duplex mode is carried out by the conditions summarized in (Table.2.). Duplex mode is different in the sense of scanning way. This mode performs continual measurement of blood perfusion in one point with sample frequency 100 Hz (step 10 ms). After selecting this mode, it is possible to control of head distance to tissue, sample frequency and change of intensity threshold.

Table 2: Controlled conditions in duplex mode.

Atmospheric pressure	101.4 kPa
Light conditions	95.5 lx
Surrounding temperature	28.5 °C
Tissue temperature	36.4 °C
Humidity	22.6 °C
Record length	9 s

For processing of results we use perfusion values and intensity from duplex mode. The measured values are related on one skin point (back of the hand), they have inclination angle 0° to 70° from parallel surface of measuring head (Fig. 7.). The fig. 8. shows graphical representation of the correction curve of perfusion change in the dependence of incidence angle. Perfusion units (PU) are approximated by quadratic model:

$$PU = a + b\theta + c\theta^2 \tag{1}$$

Parameter  $\theta^2$  is approximated by the confidence interval:  $\{-0.0136312; 0.036515\}$  containing zero point, and p-value: 0.293605 which is greater than 0.05. On the base of the results, for this case the parameter  $\theta^2$  is negligible against rest of the values. After recalculation of values for the linear equation:

$$PU = a + b\theta \tag{2}$$

We obtain the linear dependence (fig. 9.). The resulting linear equation is expressed by the following way:

$$PU = 348.74 - 3.31619\theta \quad (3)$$

This formulation consist the main part of the final perfusion recalculation  $PU_{measured}$  to  $PU_{true}$ . The white line led by the center of the correction graph determines the linear correction curve. The dark gray band around the correction curve consists of 95% probability of value occurrence in the measured point.

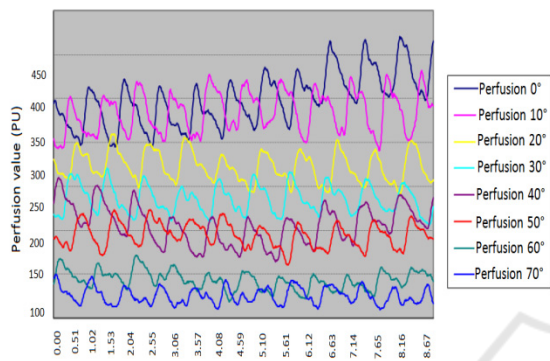


Figure 7: 9 second perfusion records in the dependence of angle.

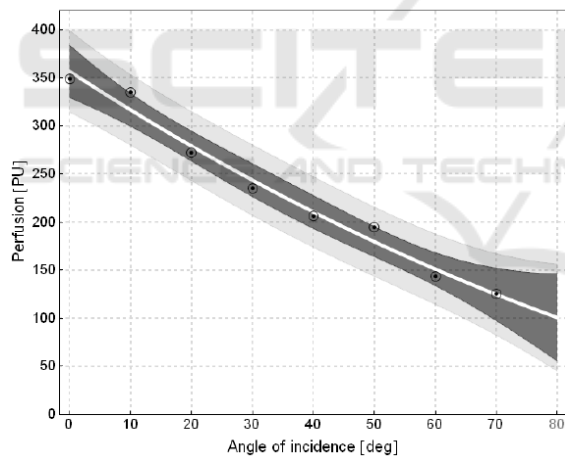


Figure 8: Perfusion change within angle change for quadratic model.

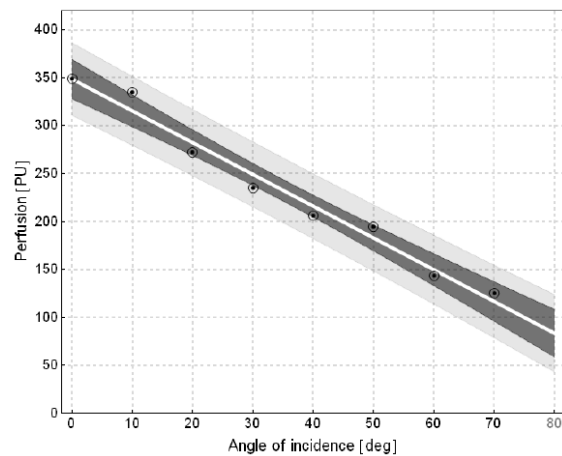


Figure 9: Perfusion change within angle change for linear model.

Equally as for imaging of the quadratic and linear model, it is approached to building of quadratic (Fig. 10.) and linear (Fig. 11.) intensity model.

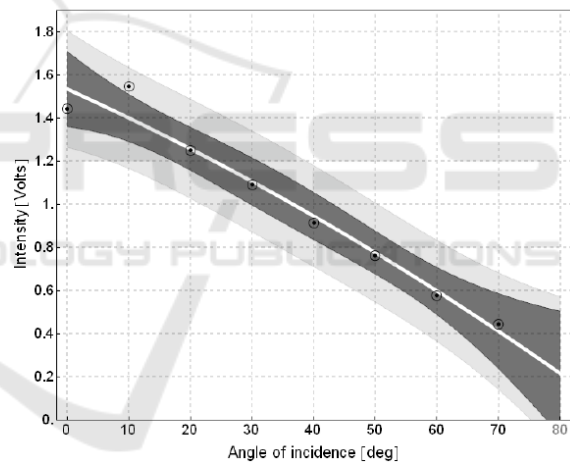


Figure 10: Intensity change within angle change for quadratic model.

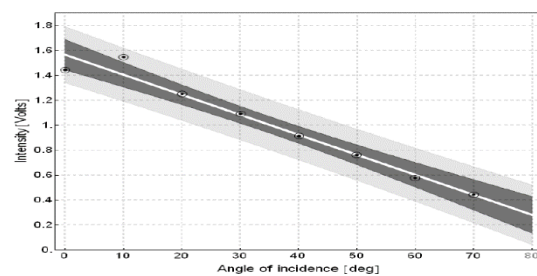


Figure 11: Intensity change within angle change for linear model.

The last effect of measured parameters is dependence of PU in the dependence of the distance. A selected location of measurement is focused on 1. A Segment of middle finger (digitus medius) measured from side of back of the hand (Fig. 12.). Consequently, we are focused on forearm (Fig. 13.). On the base of statistical values of the linear models, it is obvious that in the distance from 10.5 to 35.5 cm effect of distance change is statistically negligible. We must state that the values of this graph are obtained from person suffering from Reynolds syndrome.

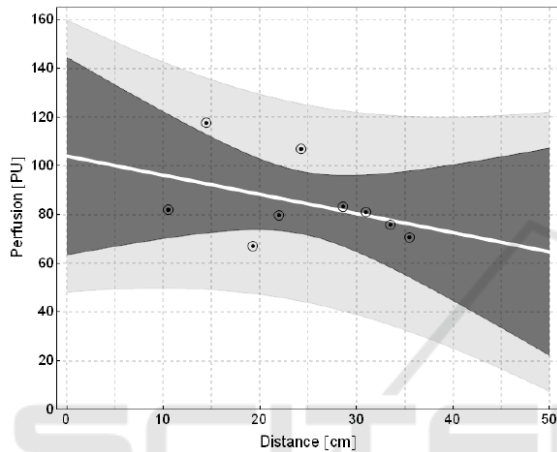


Figure 12: Intensity change within angle change for linear model.

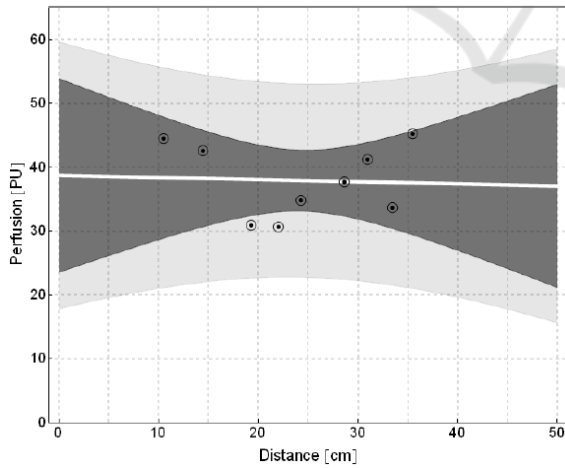


Figure 13: Perfusion change within distance change for linear model „Forearm“.

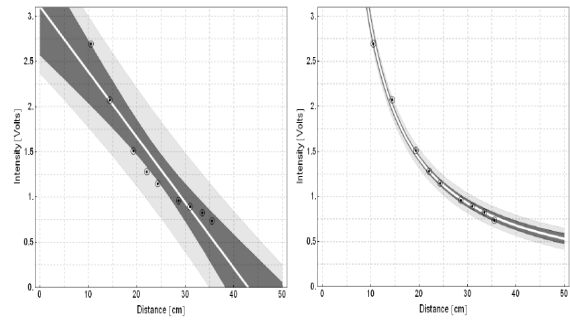


Figure 14: Intensity change within distance change for linear model „middle finger“ and their inverse quadrat.

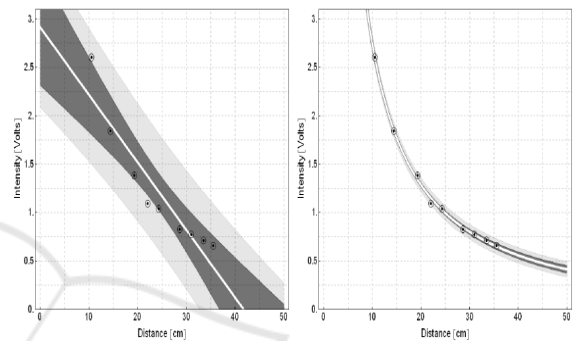


Figure 15: Intensity change within distance change for linear model „forearm“ and their inverse quadrat.

### 4.3 Theoretical Proposal of Curvature Correction Influence

The reference plane is placed perpendicularly to axes of measuring head in distance  $r_0$  from the reference point of head  $H$ . Particularly for PeriScan PIM3 it is  $r_0 = 25\text{ m}$ . A laser beam comes from deeper place of head – point  $S$ , whose distance from reference plane is  $r_s > r_0$ . It comes from the calibration curve (rather from calibration line).

The Cartesian coordinates system is fitted by  $z$  axis to axis of head, where orientation of  $z$  axis is equal with outgoing laser beam direction. The  $x$  and  $y$  axes are oriented in parallel with lines connecting of laser beam intersection with reference plane (in the scanning positions). The beginning of the coordinate system is denoted by  $\theta$ , intersection of head axis with measured area is denoted by  $Q$ . A laser beam outgoing from (virtual) point  $S$  is swept by the way that in the moment of measurement in reference plane it pass through points with coordinates  $(u, v, \theta)$ , one such point is denoted as  $R$  (Fig. 16.). These points consist the regular grid with sides  $d_u$  and  $d_v$ .

If we have perfusion calibration curve for incidence angle correction, we have:

$$PU_{true} = PU_{measured} \cdot f(\theta) \quad (4)$$

, respectively directly for cos function we have:

$$PU_{true} = PU_{measured} \cdot g(\cos\theta) \quad (5)$$

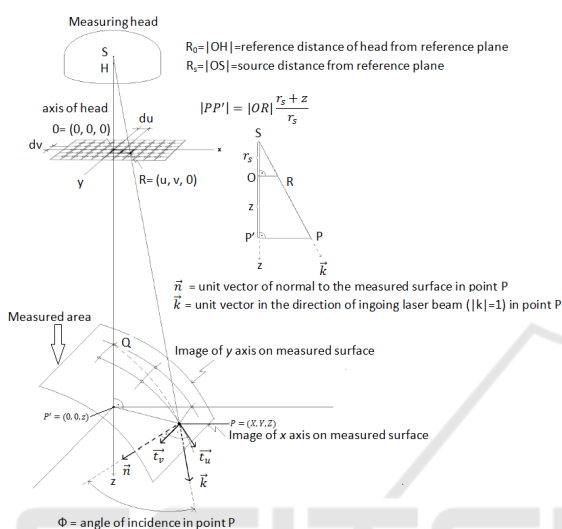


Figure 16: Proposed situation of measurement correction.

On the base of the perfusion map  $PU_{measured}[i, j]$  and the incidence angle map  $\theta[i, j]$  (respectively  $\cos\theta[i, j]$ ) we can determine perfusion map corrected on incidence angle  $PU_{true}[i, j]$  on the base of the equation 5.

## 5 CONCLUSIONS

Before performing practical measurement, it was necessary to add markers of tentative angles to stabilizing arm. The arm performs stabilization only of arm area of interest. Before performing of each measurement, the surrounding conditions of experiment were recorded in which experiment can be repeated.

The results from single mode exhibit differences in imagined areas. In the fact the imagined tissue in dermis layer has same microcirculation of blood elements, but measurement under different angle showed that the device is affected by personally unaffected influences distorting measurement results. Consequences of this angle change were observable on Duplex mode. Under perpendicular

angle of laser beam to tissue, laser beam goes through the thinnest thickness of epidermis layer, and direction of major number of blood elements is predominantly forward and reverse. Any scanning of skin under different angle than perpendicular cause greater absorption of laser beam, because trajectory of laser beam intersection is extended. Furthermore, blood element movement is detected under certain angle  $\alpha$ . The correction curve created in the Duplex mode shows the particular dependence of PU change on angle change. For using of correction curve (linear characteristic) to any measured area, it was necessary to put measured curve values to ratio with stable part of linear characteristic.

Within making of the theoretical procedure, it was found out that PeriScan PIM3 together with software do not have sufficient equipment which would be able to measure of each perfusion matrix discrete point. There are three reasons why it was not possible to make experiments with the device. It is only one device utilized for acute burn states, for determining of proper diagnosis uses non-invasive diagnostic method, and it does not belongs to commonly used devices and the device must have been acquired from own budget of University hospital in Ostrava. Nevertheless, the theoretical model conception is relatively strongly depended on this feature. All other acquired records are sufficient to correction of discretely values  $PU_{measured}$  transformation on real values  $PU_{true}$ .

## ACKNOWLEDGEMENTS

This article has been supported by financial support of TA ČR ,PRE SEED Fund of VSB-Technical univerzity of Ostrava/TG01010137. The work and the contributions were supported by the project SV4506631/2101 'Biomedicinské inženýrské systémy XII'.

## REFERENCES

- Augustynek, M., Labza, Z., Penhaker, M., Korpas, D., & Society, I. C. (2010). *Verification of set up dual-chamber pacemaker electrical parameters*. 2010 Second International Conference on Computer Engineering and Applications: Icccea 2010, Proceedings, Vol 2, 168-172. doi:10.1109/iccea.2010.187
- Basak, K., Dey, G., Mahadevappa, M., Mandal, M., Sheet, D., Dutta, P.K. 2016. *Learning of speckle statistics for in vivo and noninvasive characterization of cutaneous wound regions using laser speckle contrast imaging*. Microvascular Research, 107, pp. 6-16.

- Bevilacqua, A., Barone, D., Baiocco, S., Gavelli, G. A. 2016. *Novel approach for semi-quantitative assessment of reliability of blood flow values in DCE-CT perfusion*. Biomedical Signal Processing and Control, 31, pp. 257-264.
- Blazek, P., Krenek, J., Kuca, K., Krejcar, O., Jun, D., & Ieee. (2015). *The biomedical data collecting system*. 2015 25th International Conference Radioelektronika (Radioelektronika), 419-422.
- Brezinova, J., Hudak, R., Guzanova, A., Draganovska, D., Izarikova, G., & Koncz, J. (2016). *Direct metal laser sintering of ti6al4v for biomedical applications: Microstructure, corrosion properties, and mechanical treatment of implants*. Metals, 6(7). doi:10.3390/met6070171.
- Cerny, M., Martinak, L., Penhaker, M., & Rosulek, M. (2008). *Design and implementation of textile sensors for biotelemetry applications*. In A. Katashev, Y. Dekhtyar, & J. Spigulis (Eds.), 14th nordic-baltic conference on biomedical engineering and medical physics (Vol. 20, pp. 194-197).
- Cerny, M., & Penhaker, M. (2009). *Circadian rhythm monitoring in homecare systems*. In C. T. Lim & J. C. H. Goh (Eds.), 13th international conference on biomedical engineering, vols 1-3 (Vol. 23, pp. 950-953).
- Goei, H., van der Vlies, C.H., Ho, M.J., Tuinebreijer, W.E., Nieuwenhuis, M.K., Middelkoop, E., van Baar, M.E. 2016. *Long-term scar quality in burns with three distinct healing potentials*. A multicenter prospective cohort study *Wound Repair and Regeneration*, 24 (4), pp. 721-730.
- Ida, T., Iwazaki, H., Kawaguchi, Y., Kawauchi, S., Ohkura, T., Iwaya, K., Tsuda, H., Saitoh, D., Sato, S., Iwai, T. 2016. *Burn depth assessments by photoacoustic imaging and laser Doppler imaging* *Wound Repair and Regeneration*, 24 (2), pp. 349-355.
- Elamin, S.E., Dickson, J.K., Mackie, I.P. 2015. *Is Laser Doppler imaging (LDI) a measure of burn depth?* *Burns*, 41 (2), p. 413.
- Klosová, H., Štětinský, J., Bryjová, I., Hledík, S. and Klein, L. 2013. *Objective evaluation of the effect of autologous platelet concentrate on post-operative scarring in deep burns*. *Burns*, DOI: 10.1016/j.burns.2013.01.020.
- Kubicek, J., Penhaker, M., Bryjova, I., & Augustynek, M. (2016). *Classification method for macular lesions using fuzzy thresholding method*. In E. Kyriacou, S. Christofides, & C. S. Pattichis (Eds.), Xiv mediterranean conference on medical and biological engineering and computing 2016 (Vol. 57, pp. 239-244).
- Kukucka, M. (2009). *Modeling of logic diagnostic system knowledge base evaluation*. Machaj, J., Brida, P., & Benikovsky, J. (2016). *Scalability optimization of seamless positioning service*. Mobile Information Systems. doi:10.1155/2016/9714080
- Majernik, J., & Jarcuska, P. (2012). *Education of clinical disciplines in pre and post-graduate study oriented on increasing of newest infectious diseases knowledge*. In A. Isman (Ed.), 3rd international conference on new horizons in education - inte 2012 (Vol. 55, pp. 604-611).
- Majernik, J., Jarcuska, P., & Ieee. (2014). *Web-based delivery of medical education contents used to facilitate learning of infectology subjects*. 2014 10th International Conference on Digital Technologies (Dt), 225-229.
- Marek, T., & Krejcar, O. (2015). *Optimization of 3d rendering in mobile devices*. In M. Younas, I. Awan, & M. Mecella (Eds.), Mobile web and intelligent information systems (Vol. 9228, pp. 37-48).
- Penhaker, M., Darebnikova, M., & Cerny, M. (2011). *Sensor network for measurement and analysis on medical devices quality control*. In J. J. Yonazi, E. Sedoyeka, E. Ariwa, & E. ElQawasmeh (Eds.), E-technologies and networks for development (Vol. 171, pp. 182-196).
- Penhaker, M., Kasik, V., & Snasel, V. (2013). *Biomedical distributed signal processing and analysis*. In K. Saeed, R. Chaki, A. Cortesi, & S. Wierzchon (Eds.), Computer information systems and industrial management, cisim 2013 (Vol. 8104, pp. 88-95).
- Simonsen, C.Z., Schmitz, M.L., Madsen, M.H., Mikkelsen, I.K., Chandra, R.V., Leslie-Mazwi, T., Andersen, G. 2016. *Early neurological deterioration after thrombolysis*. Clinical and imaging predictors () *International Journal of Stroke*, 11 (7), pp. 776-782.
- Schindler, T.H. 2016. *Myocardial blood flow*. Putting it into clinical perspective (*Journal of Nuclear Cardiology*, 23 (5), pp. 1056-1071).
- PERIMED AB, 2008. *PeriScan PIM3 System – Extended User Manual*, July retrieved 2012, URL <http://www.perimed-instruments.com/>.
- Shin, Y., Yi, H.S. 2016. *Diagnostic accuracy of laser Doppler imaging in burn depth assessment*. Systematic review and meta-analysis *Burns*.
- Stetinsky, J., Klosova, H., Kolarova, H., Salounova, D., Bryjova, I., & Hledik, S. (2015). *The time factor in the ldi (laser doppler imaging) diagnosis of burns*. *Lasers in Surgery and Medicine*, 47(2), 196-202. doi:10.1002/lsm.22291
- Thieme, D., Spilker, G., Lefering, R., Weinand, C. 2016. *O2C Laser Doppler and Digital Photo Analysis for Treatment Evaluation of Beta-Glucan versus Provitamin Pantothenic Acid of Facial Burns* *Facial Plastic Surgery*, 32 (2), pp. 225-231.